

# Good views of the Galaxy

Hiranya V. Peiris

Princeton University Observatory, Peyton Hall, Princeton, NJ 08544;  
hiranya@astro.princeton.edu

## ABSTRACT

Fitting Galactic structure models to star counts only provides useful information about the Galaxy in some directions. In this paper, we investigate the use of  $\chi^2$  goodness-of-fit tests to discriminate between degenerate Galactic structure models, and the implications of this technique for the Galactic spheroid and thick disk components. The axis ratio of the Galactic spheroid and the normalization of spheroid stars with respect to disk stars introduce a degenerate effect which means that Galactic structure models with certain combinations of these parameters are indistinguishable from each other in most directions. We present an analysis of the optimal directions in which these degeneracies can be lifted. Poisson and magnitude errors are taken into account, and an attempt is made to place an upper limit on the systematic error due to separation of spheroid stars from thick/old disk stars. We find that the magnitude range  $20 < V < 21$  is the best for lifting most degeneracies, and present the optimal combinations of directions using which this can be achieved. We also give directions in which the signature of the presence of a Galactic thick disk can be most readily identified, and the directions in which contamination from a thick disk can be minimized. It is hoped that forthcoming data from large-scale sky surveys would reveal much about the structure of our Galaxy using star count techniques.

*Subject headings:* Galaxy: structure — stars: statistics

## 1. Introduction

Since we observe our Galaxy from within it, we must use indirect tools such as star counts to probe its structure. The success of this method relies on assuming that the components of the Milky Way Galaxy have stars distributed similarly to those of galaxies of the same Hubble type, and comparing models with observations only in regions where little

obscuration is known to be present. Observed “star counts” (i.e. the distribution of number counts of stars in apparent magnitude and color within a given area/direction in the sky) are then used to determine parameters in distribution functions whose overall shapes are assumed known.

Within the past two decades, Galactic structure models of varying degrees of complexity have been developed (Bahcall & Soneira, 1980, 1981, 1984, Gilmore 1984, Robin and Cr ez e 1986a, 1986b, Reid & Majewski 1993). However, during the same period, relatively few sets of observational star count data have been published.

Galactic structure models, for a given set of structure parameters, typically predict differential number counts (stars / apparent magnitude bin / area) and frequency-color distributions (stars / color bin / area) for a specified direction. Because the Galaxy consists of at least two components, obeying different density laws and being characterized by different stellar populations, these distributions change with the color range, magnitude range and direction under consideration. It is important to match both the shapes of these distributions and the absolute numbers of stars with observations.

Existing models predict differential number counts reasonably well, to faint magnitudes of  $V \sim 21$ , but recent studies suggest that agreement between observed and predicted frequency-color distributions breaks down at faint magnitudes below  $V \sim 19$  (Reid & Majewski 1993). “Standard” Galactic structure models appear to overestimate the contribution of (blue) spheroid stars substantially, and the contribution of (red) disk stars is correspondingly underestimated in order to match the total number counts. Contrary to prediction, observations show that *disk* stars are the majority population to at least  $V \sim 21$ . However, the small sizes of fields in which data are available mean that comparisons in frequency-color space are complicated by uncertainties due to small-number statistics.

A further hindrance to the determination of distribution function parameters arises due to the fact that data are only available in a small number of directions. This presents a problem in trying to fit model parameters which cause degenerate effects in the number counts. For instance, increasing the normalization of the Galactic spheroid and decreasing its axis ratio  $b/a$  (or vice versa) represents a degeneracy. This means that in most directions, one cannot distinguish between models with a flattened spheroid plus a low normalization ratio of spheroid stars to disk stars, and those with a high axis ratio plus a high normalization.

We anticipate the availability of star count data from large-scale, deep sky surveys in the near future (see § 3 and § 5) which would solve the problem of excessive statistical noise, and provide data in almost any direction we desire. In this paper, we investigate the

possibility of tackling the degeneracy problem by attempting to find two or more directions in which  $\chi^2$  goodness-of-fit tests can distinguish between spheroid parameter combinations that yield degenerate results in general.

A degenerate situation is defined as one in which, in a general direction, there is no significant difference in results given by a model where a pair of spheroid parameters are characterized by values  $(p, q)$  and a model characterized by values  $(r, s)$ . This means that one cannot learn very much about these spheroid parameters even if these models fit the spheroidal star counts in that direction with reasonable accuracy. The degenerate parameters we examine here are the spheroid axis ratio and the normalization of spheroid stars to disk stars in the solar neighborhood.

By using  $\chi^2$  tests with a specified set of directions as “bins” (see e.g. Press et al. 1992), we have investigated the optimal directions for breaking this degeneracy. These tests are based on fitting the total number of spheroid stars in each direction “bin”, for a given set of directions and a particular magnitude range. Therefore, both the observed number count and color information is used, since the spheroid counts have to be separated from the total counts using the frequency-color distribution, as explained in § 4.1.4.

§ 2 describes the Galactic structure models we have used in these tests. Details of the directions used in the analysis are found in § 3. A description of the  $\chi^2$  tests, along with our results, are presented in § 4. We conclude, in § 5, that there are two or more directions in which most “degenerate” model pairs can be distinguished. We find the magnitude range  $20 < V < 21$  to be the most useful for this purpose. We also make suggestions for the best directions in which to separate spheroidal stars from old- and thick-disk stars using a frequency-color distribution diagram, and conversely, the directions in which the presence of a thick disk would be most clearly observed.

## 2. The Models

While it is our intention to illustrate the use of this technique in general, for specificity we will use the model that is usually referred to in the literature as the Bahcall-Soneira (B&S) model. We have taken the realization of the B&S model in the form of the Export Code that is available on the Internet (<http://www.sns.ias.edu/~jnb/Html/galaxy.html>). This model is described in Bahcall (1986). We have added a few refinements as described below.

The disk luminosity function (LF) has been modified between  $9.5 < M_V \leq 18.0$  to match the LF recently derived from *Hubble Space Telescope* (*HST*) M dwarfs (Figure 2,

Gould et al. 1997). A “sech<sup>2</sup>” model has been used for the vertical density distribution function of main sequence disk stars in the same absolute magnitude range, as given in Eq. 3.2 of the same work. The HST LF was derived using two different methods: a maximum likelihood (ML) fit that takes into account both measurement errors and Malmquist bias, and a naive binning method where the total number of stars in a given magnitude bin is divided by the effective volume integrated over that bin. This binning method takes into account neither Malmquist bias nor observational error. The two alternative derivations agree quite well over most of the LF, but at the faint end ( $13.5 \leq M_V \leq 18.5$ ) the ML procedure could be affected by a statistical fluctuation. Because Poisson errors are potentially a much more serious problem at the faint end than Malmquist bias (since the HST survey extends to the “top” of the disk), we choose to use the form of the LF derived using the binning method.

The spheroid LF has been modified between  $7.5 \leq M_V \leq 13.5$  to match another LF derived from *HST* star counts (Figure 3, Gould et al. 1998). Note that this LF differs in its zero point by a factor of  $\sim 2$  with studies of kinematically-selected local spheroid subdwarfs (Dahn et al. 1995).

The disk and spheroid LFs used are shown in Figure 1. In addition to the spheroidal parameters whose values are described in § 4, the color-magnitude diagram (CMD) of M13 was adopted for the spheroid CMD.

In addition to this two-component model, a three-component model was created with the addition of a thick disk with a scale height of 1200 pc, a 47 Tuc-like CMD, a disk-like LF, and a normalization to disk counts at the solar neighborhood of 2%. This was used in analyzing the separation error in identifying spheroid counts from disk/thick-disk counts using frequency-color diagrams, as described in § 4.1.4.

The density laws used for the old disk, the spheroid and the thick disk are summarized in Table 1, which also gives the normalizations used.

### 3. The Directions

We selected a representative set of directions in which to carry out the analysis, which are shown in Table 2.

Directions 1 & 2 were selected following a quantitative analysis of directions in the ( $l^{II} = 0^\circ \rightarrow 180^\circ$ ) and ( $l^{II} = 90^\circ \rightarrow 270^\circ$ ) planes, as the optimal directions in which to distinguish between the effects of the normalization and the axis ratio of the

spheroid. Bahcall and Soneira (1980) explain why these planes are especially important for determining the characteristics of the spheroid. We ran the model at  $5^\circ$  intervals in  $b^I$  in each of these planes, and calculated the variation with  $b^I$  of the ratio of spheroid counts to disk counts, and the ratio of spheroid counts for pairs of near-degenerate models: for example, using the notation (disk : spheroid normalization ratio, spheroid axis ratio),  $(800 : 1, 1.0) : (500 : 1, 0.8)$ . We then looked for directions with a high spheroid : disk ratio (in order to minimize the Poisson error in total spheroid counts as well as the error due to contamination of spheroid counts by disk stars) while at the same time, maximizing the quantity  $|(800 : 1, 1.0) : (500 : 1, 0.8) - 1|$ . Directions 1 & 2 optimized both these quantities.

Directions 3–10 were selected because fields in these directions are being prepared by the Digital Palomar Observatory Sky Survey (DPOSSII; S. G. Djorgovski & S. C. Odewahn 1998, private communication; Djorgovski et al. 1997, 1998) for star count studies. It would then be possible to see how the techniques discussed here in a theoretical sense work in practice.

#### 4. $\chi^2$ Analysis

The  $\chi^2$  statistic is

$$\chi^2 = \sum_{dir=1}^N \frac{[A_{model}(m_1, m_2, l, b)d\Omega - A_{observed}(m_1, m_2, l, b)d\Omega]^2}{\sigma^2}, \quad (1)$$

where  $dir = (l, b)$  is a given direction,  $A(m_1, m_2, l, b)d\Omega$  is the total number of spheroid stars with apparent magnitudes in the range  $m_1 \leq m \leq m_2$  in the direction  $(l, b)$  per projected sky area  $d\Omega$ , and  $\sigma$  is the error, which can have several components as described below. Reduced  $\chi^2$  is given by  $\chi^2/\nu$  where  $\nu$  is the number of degrees of freedom, in this case equal to the number of directions  $N$  (i.e. the total predicted counts are *not* renormalized to the same total counts as the data). A large value of reduced  $\chi^2$  indicates that the null hypothesis that the  $A_{observed}$ 's are drawn from the same population as the  $A_{model}$ 's is rather unlikely.

Since we do not currently have observed number counts in all the directions, we picked one model out of the set covering the investigated parameter-space to be the “observed” number counts and compared it against each of the rest of the models in the set (which represented the “theory”). The process was then repeated till each of the models had been picked as the one representing actual data.

We define the criterion for lifting the degeneracy of spheroid parameters as obtaining the probability of finding a value of reduced  $\chi^2$  greater than or equal to the “observed” value  $< 10^{-5}$ . That is, we aim to reject the null hypothesis (that the “observed” and “theoretical” models are the same) at a confidence level of 0.001%. The range of models we used spanned the parameter space (*disk : spheroid normalization ratio*)  $\times$  (*spheroid axis ratio*) = (500 : 1,800 : 1)  $\times$  (1.0, 0.8, 0.6, 0.4). Thus there are 56 possible pairings of models picked as “observed” and “theoretical”.

$\chi^2$  tests were carried out using the set of directions detailed in § 3 as “bins.” The directions yielding the highest contribution to the  $\chi^2$  value were noted as the optimal directions to use for breaking the degeneracy. It was then checked whether  $\chi^2$  tests using just those optimal directions as bins would cause the degeneracy to be lifted.

The error term  $\sigma$  can have contributions from Poisson error, magnitude error, and the systematic “separation error” which arises because spheroid stars cannot be separated cleanly from old/thick disk stars in observations, thereby introducing an error into the total spheroid counts. In general, a magnitude error of order  $\sim 0.1^{mag}$  contributes less to the error budget than the Poisson error. In a “good” direction, the separation error should contribute the least to the error budget and the number counts are Poisson-noise-limited. In a “bad” direction, the separation error can be by far the greatest source of uncertainty. In § 4.1, we first consider the case where the spheroid counts *can* be cleanly separated, and then in § 4.2 we consider the effect of adding the separation error.

#### 4.1. Analysis excluding separation error

$\chi^2$  tests were first carried out using the two-component (spheroid + old disk) model, taking into account the Poisson error of the counts and a magnitude error of  $0.1^{mag}$ , but assuming that spheroid stars can be separated cleanly from old/thick disk stars in observations.

The magnitude error was calculated as follows. Let  $N(m_1 \leq m \leq m_2)$  represent the total spheroidal number counts for apparent magnitude range  $m_1 \leq m \leq m_2$ , and let the error in the zero-point be  $\delta m$ . Then we calculate  $N_+(m_1 + \delta m \leq m \leq m_2 + \delta m)$  and  $N_-(m_1 - \delta m \leq m \leq m_2 - \delta m)$ . The error in the total spheroidal number counts due to the zero-point error in magnitude is then given by  $Max(|N - N_+|, |N - N_-|)$ .

#### 4.1.1. Directions 1 & 2

Directions 1 and 2 in Table 2 were found to be the best overall for discriminating between ordinarily degenerate models using  $\chi^2$  tests.

Using the notation [(*model taken as observation*), (*model taken as prediction*)], almost all model pairings were distinguishable from each other in the apparent magnitude range  $19 < V < 20$ . The exceptions were [(500 : 1, 0.8), (800 : 1, 1.0)] and [(800 : 1, 1.0), (500 : 1, 0.8)]. Upon examining the range  $20 < V < 21$  the degeneracy of these model pairings were also lifted, while the other model pairings also remained non-degenerate.

#### 4.1.2. Directions 3–10 ( $19 < V < 20$ )

Considering the directions 3–10 which are being prepared by the DPOSSII survey,  $\chi^2$  tests in directions 3 and 4 in apparent magnitude range  $19 < V < 20$  can distinguish between all model pairings with the exceptions shown in Table 3.

#### 4.1.3. Directions 3–10 ( $20 < V < 21$ )

Considering the model pairings in the apparent magnitude range  $20 < V < 21$  in the DPOSSII directions,  $\chi^2$  tests can distinguish between all model pairings in directions 3 and 4 except for those shown in Table 4.

#### 4.1.4. Discussion

Observationally, spheroid stars can be separated from old/thick disk stars using the bi-modal distribution that appears in star color-frequency profiles in certain directions at faint magnitude ranges. The blue and red peaks consist of spheroid and disk stars, respectively. This distribution has been interpreted as arising because the disk and spheroid components have different density gradients in a magnitude-limited survey (Bahcall & Soneira 1980). The sharp density gradient in the disk for directions far from the Galactic plane favors relatively nearby and intrinsically faint (red) stars at faint apparent magnitudes. Conversely, the shallow density gradient in the spheroid favors relatively distant, intrinsically bright (blue) stars at the same faint apparent magnitudes, because the effective volume increases at large distances.

$18 \leq V \leq 22$  is the apparent magnitude range where this double-peaked distribution is most pronounced, enabling the cleanest separation of spheroidal stars in observations (Bahcall & Soneira 1980, Reid & Majewski 1993). In this interval, the spheroid counts peak at  $B - V \sim 0.5$ , with a narrow range in color. This corresponds roughly to the main-sequence turn-off, at  $M_V \sim 4.5$ . For a given apparent magnitude interval  $m_1 \leq m \leq m_2$ , only stars within a range of absolute magnitudes  $M_1 \leq M \leq M_2$  contribute to the observed number counts. The majority contribution to the blue spheroidal peak comes from stars near the main sequence turn-off, with  $+4 \leq M_V + 6$  (corresponding to  $\sim 0.5 \rightarrow 1.0 M_\odot$ ). Evolved stars with  $M_V \leq 3.5$  make negligible contribution to deep star counts at this magnitude range.

The shallow density gradient in the spheroid leads to a broad distribution of number counts with distance in a given direction, peaking at  $\sim 7$  kpc in the direction of the North Galactic Pole (Bahcall & Soneira 1980). Therefore, the fainter the magnitude range under consideration, the better the performance of the  $\chi^2$  statistic, because spheroid number counts are still rising at  $V \sim 22$ . Thus the Poisson errors and magnitude errors at fainter magnitudes are smaller. This is the reason that the magnitude range  $20 \leq V \leq 21$  is more useful for lifting degeneracies using the  $\chi^2$  tests than the brighter range  $19 \leq V \leq 20$ . Once we go even fainter to the range  $21 \leq V \leq 22$ , photometric uncertainties and observational errors, such as star-galaxy separation and contamination of the blue spheroidal population by quasars and compact emission line galaxies (CELGs) increasingly start to affect counts. Thus the intermediate apparent magnitude range  $20 \leq V \leq 21$  is the optimal one to use for the purpose of lifting degeneracies by this method.

## 4.2. Analysis including separation error

Figures 2 and 3 show frequency distributions of star colors for a particular “standard” model, in the ten directions given in Table 2, for magnitude ranges  $19 < V < 20$  and  $20 < V < 21$ . The maximum error in separating out the spheroid stars arises if there is a thick disk component which tends to fill up the valley between the double-peaks due to spheroid and old disk stars, or in the worst cases, peaks within the blue spheroid peak. The separation error is calculated as the area under the blue peak in total (spheroid + old disk + thick disk) counts, minus the calculated (i.e. model) spheroid counts. The “blue peak” is taken to be bounded on the red side by the color corresponding to the minimum point of the total counts.

Now, we consider the effect of including the systematic error due to separating spheroid stars from old/thick disk stars in observations, using the three-component (spheroid + old



disk + thick disk) model. The separation error is an overestimate since this contamination in observations can be corrected for to some extent by subtracting model disk counts from the total counts.

The contamination due to the thick disk was found to dominate that due to old disk stars in all cases. This error was found to be smaller in the apparent magnitude range  $20 < V < 21$  than in the range  $19 < V < 20$ . Hence the following analysis was only carried out for the fainter range. Further, since the ratio of separation error to total spheroid counts increases significantly for models with smaller axis ratios, the models with axis ratio 0.4 were excluded from the analysis. Thus, model parameter space was restricted to  $(500 : 1, 800 : 1) \times (1.0, 0.8, 0.6)$ .

Upon including the separation error, directions 1 and 2, found to be the best overall in discriminating between model parameters, were found to be virtually useless, since the thick disk counts peaked within the spheroid peak for these directions.

In the case of the DPOSSII directions (3–10), all the model pairings which could be distinguished in this apparent magnitude range using  $\chi^2$  tests in directions 3 and 4 remained non-degenerate, except  $[(800 : 1, 0.6), (500 : 1, 0.6)]$ , which became degenerate. The rest of the model pairings which had been non-degenerate in directions given in Table 4 also became degenerate.

Table 5 shows whether these degenerate models can be discriminated using other combinations of directions.

During this analysis, it was found directions 7 and 9 are generally good for minimizing the effects due to the thick disk. Conversely, directions 1 and 10 are particularly good for looking for the presence of the thick disk.

## 5. Conclusions

We found that directions 1 ( $l^{II} = 0^\circ, b^{II} = 40^\circ$ ) and 2 ( $l^{II} = 90^\circ, b^{II} = 40^\circ$ ) in apparent magnitude range  $20 < V < 21$  were the most effective in distinguishing between effects due to degenerate parameters, assuming that spheroid stars could be separated cleanly from disk and thick-disk stars.

In the case that the maximum possible separation error (i.e. uncorrected for disk and thick disk counts) was included in the analysis, directions 3 (the North Galactic Pole) and 4 ( $l^{II} = 67^\circ, b^{II} = 49^\circ$ ) in apparent magnitude range  $20 < V < 21$  were the most useful. In those models where these directions failed to lift the degeneracy, directions

7 ( $l^{II} = 111^\circ, b^{II} = -46^\circ$ ) and 9 ( $l^{II} = 172^\circ, b^{II} = 48^\circ$ ) were the best for minimizing contamination from the thick disk, which dominates the separation error.

Directions 1 ( $l^{II} = 0^\circ, b^{II} = 40^\circ$ ) and 10 ( $l^{II} = 61^\circ, b^{II} = -37^\circ$ ) were found to be the most effective in detecting the presence of a thick disk.

This is an exciting time in which deep, high-quality data-sets covering large areas of the sky are about to become available from much-anticipated surveys such as the Sloan Digital Sky Survey (SDSS, see e.g. Gunn & Knapp 1993, Gunn & Weinberg 1995) and the DPOSSII (see § 3 for references). The use of survey data for star count studies is complicated by the fact that many existing “standard” Galactic structure models are based on color-magnitude diagrams (CMDs) and luminosity functions (LFs) determined in the standard Johnson-Morgan-Cousins  $UBV$  photometric system, and are only useful for comparison with data in the visual band or in photometric systems to which accurate transformations exist. However, in cases such as that of the SDSS, which uses the non-standard  $u'g'r'i'z'$  photometric system (Fukugita et al. 1996), such models will soon be re-created using LFs and CMDs determined in the SDSS photometric bands. The DPOSSII uses three photographic  $JFN$  bands calibrated to the Gunn  $gri$  bands. Though these are different from the photoelectric/CCD  $gri$  bands (Palomar, 4-Shooter, SDSS) they are well-defined. Once the work of creating a model based on the SDSS bands is completed, it should be fairly straightforward to translate the stellar sequences and LFs to the DPOSSII  $gri$  bands. Until such models are available, a different approach to star count models, such as the evolutionary stellar population synthesis technique (Fan 1999) can be used.

The possibility of fitting models simultaneously in a multitude of directions with large samples containing number, magnitude and color information should revolutionize studies of Galactic structure using star counts.

The author is very grateful to John Bahcall for his helpful advice. She wishes to thank Andy Gould for providing machine-readable versions of Figure 2 of Gould et al. (1997) and Figure 3 of Gould et al. (1998); David Spergel and Xiaohui Fan for instructive discussions on Galactic Structure models; and Mark Jackson for useful comments on the manuscript.

Table 1. The Assumed Stellar Distributions.

Component	Distribution
Disk	$n_D = n_D(R_0) \exp[-z/H(M_V)] \exp[-(x - R_0)/h]$
Spheroid	$n_{sph} = n_{sph}(R_0)(R/R_0)^{-7/8} \exp[-10.093(R/R_0)^{1/4} + 10.093]$ $\times 125(R/R_0)^{-6/8} \exp[-10.093(R/R_0)^{-1/4} + 10.093]$ , $R < 0.03R_0$ $\times [1 - 0.08669/(R/R_0)^{1/4}]$ , $R \geq 0.03R_0$
Thick Disk	$n_{TD} = n_{TD}(R_0) \exp[-z/H_{TD}] \exp[-(x - R_0)/h]$
Normalization	$n_D(R_0) = 0.13pc^{-3}$ , $n_{TD}(R_0) = 0.0026pc^{-3}$ , $n_{sph}(R_0) = 0.00026pc^{-3}$ or $0.0001625pc^{-3}$ depending on model

Note. — Here  $z$  is the distance perpendicular to the plane,  $x$  is the galactocentric distance in the plane, and  $h$  is the old disk scale length. Galactocentric distance  $R = (x^2 + z^2/\kappa^2)^{1/2}$ , where  $\kappa$  is the axis ratio and  $1 - \kappa$  is the ellipticity. We adopt  $R_0 = 8$  kpc and  $h = 3.5$  kpc. The old disk scale height  $H(M_V)$  is given in Bahcall and Soneira (1980). The thick disk is taken to have a scale height  $H_{TD} = 1.2$  kpc and a 47-Tuc-like CMD.

Table 2. A Representative Set of Directions.

Direction	$l^{II}(1950)$	$b^{II}(1950)$	Comments <sup>a</sup>
1.....	0°	+40°	BS9 <sup>b</sup>
2.....	90	+40	Between BS4 and BS7 <sup>b</sup>
3.....	...	+90	Galactic pole (SA57, BS1) <sup>c,d</sup>
4.....	67	+49	BS16 <sup>c,d</sup>
5.....	180	+50	BS6 <sup>c</sup>
6.....	180	+30	BS8 <sup>c</sup>
7.....	111	–46	BS11, SA68 <sup>c</sup>
8.....	167	–51	BS13 <sup>c</sup>
9.....	172	+48	BS14 <sup>c</sup>
10.....	61	–37	BS17 <sup>c</sup>

<sup>a</sup>The field identification BS*n* denotes the designation assigned to a given direction in Table 1 of Bahcall and Soneira (1981), where quantities that can be efficiently studied in that direction are listed. The Selected Area number is also given for fields which have been studied.

<sup>b</sup>These directions were determined to be the best for distinguishing between effects due to spheroid flattening and normalization using the two-component (old disk + spheroid) standard model.

<sup>c</sup>These fields are being made available by the DPOSSII survey for star count studies.

<sup>d</sup>These directions were determined to be the best for determining the spheroid parameters out of the DPOSSII directions.

Table 3. Model pairings degenerate in directions 3 and 4 for  $19 < V < 20$  excluding separation error.

Model pairing <sup>a</sup>	Min. directions required to lift degeneracy
[(500 : 1, 0.8), (800 : 1, 1.0)]	6, 7
[(800 : 1, 1.0), (500 : 1, 0.8)]	6, 7, 10
[(500 : 1, 0.6), (800 : 1, 0.8)]	... <sup>b</sup>
[(800 : 1, 0.8), (500 : 1, 0.6)]	... <sup>b</sup>
[(500 : 1, 0.4), (800 : 1, 0.6)]	... <sup>b</sup>
[(800 : 1, 0.4), (500 : 1, 0.4)]	4, 10

<sup>a</sup>Uses notation  $[(model\ taken\ as\ observation), (model\ taken\ as\ prediction)]$ .

<sup>b</sup>This model pairing cannot be distinguished using the DPOSSII directions 3–10 in the apparent magnitude range  $19 < V < 20$ .

Table 4. Model pairings degenerate in directions 3 and 4 for  $20 < V < 21$  excluding separation error.

Model pairing <sup>a</sup>	Min. directions required to lift degeneracy
[(500 : 1, 0.8), (800 : 1, 1.0)]	6, 10
[(800 : 1, 1.0), (500 : 1, 0.8)]	6, 10
[(500 : 1, 0.6), (800 : 1, 0.8)]	3, 6
[(800 : 1, 0.8), (500 : 1, 0.6)]	... <sup>b</sup>

<sup>a</sup>Uses notation [(*model taken as observation*), (*model taken as prediction*)].

<sup>b</sup>This model pairing cannot be distinguished using the DPOSSII directions 3–10 in the apparent magnitude range  $20 < V < 21$ .

Table 5. Model pairings degenerate in directions 3 and 4 for  $20 < V < 21$  including separation error.

Model pairing <sup>a</sup>	Min. directions required to lift degeneracy
[(500 : 1, 0.8), (800 : 1, 1.0)]	7, 9
[(800 : 1, 1.0), (500 : 1, 0.8)]	... <sup>b</sup>
[(500 : 1, 0.6), (800 : 1, 0.8)]	... <sup>b</sup>
[(800 : 1, 0.8), (500 : 1, 0.6)]	... <sup>b</sup>
[(800 : 1, 0.6), (500 : 1, 0.6)]	7, 9

<sup>a</sup>Uses notation [(*model taken as observation*), (*model taken as prediction*)].

<sup>b</sup>This model pairing cannot be distinguished using the DPOSSII directions 3–10 in the apparent magnitude range  $20 < V < 21$  using  $\chi^2$  tests including the separation error.

## REFERENCES

- Bahcall, J. N., & Soneira, R. M. 1980, *ApJS*, 44, 73
- Bahcall, J. N., & Soneira, R. M. 1981, *ApJS*, 47, 357
- Bahcall, J. N., & Soneira, R.M. 1984, *ApJS*, 55, 67
- Bahcall, J. N. 1986, *ARA&A*, 24, 577
- Dahn, C. C., Liebert, J. W., Harris, H., & Guetter, H. C. 1995, *ESO Workshop on the Bottom of the Main Sequence and Beyond*, ed. C. G. Tinney (Heidelberg: Springer), 239
- Djorgovski, S. G., de Carvalho, R. R., Odewahn, S. C., Gal, R. R., Roden, J., Storolz, P., & Gray, A. 1997, *Applications of Digital Image Processing XX*, ed. Tescher, *proc. S.P.I.E.* 3164
- Djorgovski, S. G., Gal, R. R., Odewahn, S. C., de Carvalho, R. R., Brunner, R., Longo, G., & Scaramella, R. 1998, to appear in *Wide Field Surveys in Cosmology*, ed. Colombi & Mellier, *proc. XIV IAP Colloq.*, in press.
- Fan, X. 1999, *AJ*, 117, 2528
- Fukugita, M., Ichikawa, T., Gunn, J. E., Doi, M., Shimasaku, K., & Schneider, D. P. 1996, *AJ*, 111(4), 1748
- Gilmore, G.F. 1984, *MNRAS*, 207, 223
- Gould, A., Bahcall, J. N., & Flynn, C. 1997, *ApJ*, 482, 913
- Gould, A., Flynn, C., & Bahcall, J. N. 1998, *ApJ*, 503, 798
- Gunn, J. E., & Knapp, G. R. 1993, in *ASP Conf. Ser. 43, Sky Surveys: Protostars to Protogalaxies*, ed. Soifer, 267
- Gunn, J. E., & Weinberg, D. H. 1995, in *Wide Field Spectroscopy and the Distant Universe*, ed. Maddox & Arag on-Salamanca, (World Scientific, Singapore)
- Press, W. H., Teukolsky, S. A., Vetterling, W. T., & Flannery, B. P. 1992, *Numerical Recipes in C (2<sup>nd</sup> Edition; C.U.P.)*
- Reid, I. N., & Majewski, S.R. 1993, *ApJ*, 409, 635
- Robin, A., & Cr ez e, M. 1986a, *A&A*, 157, 1



Robin, A., & Crézé, M. 1986b, *A&AS*, 64, 53

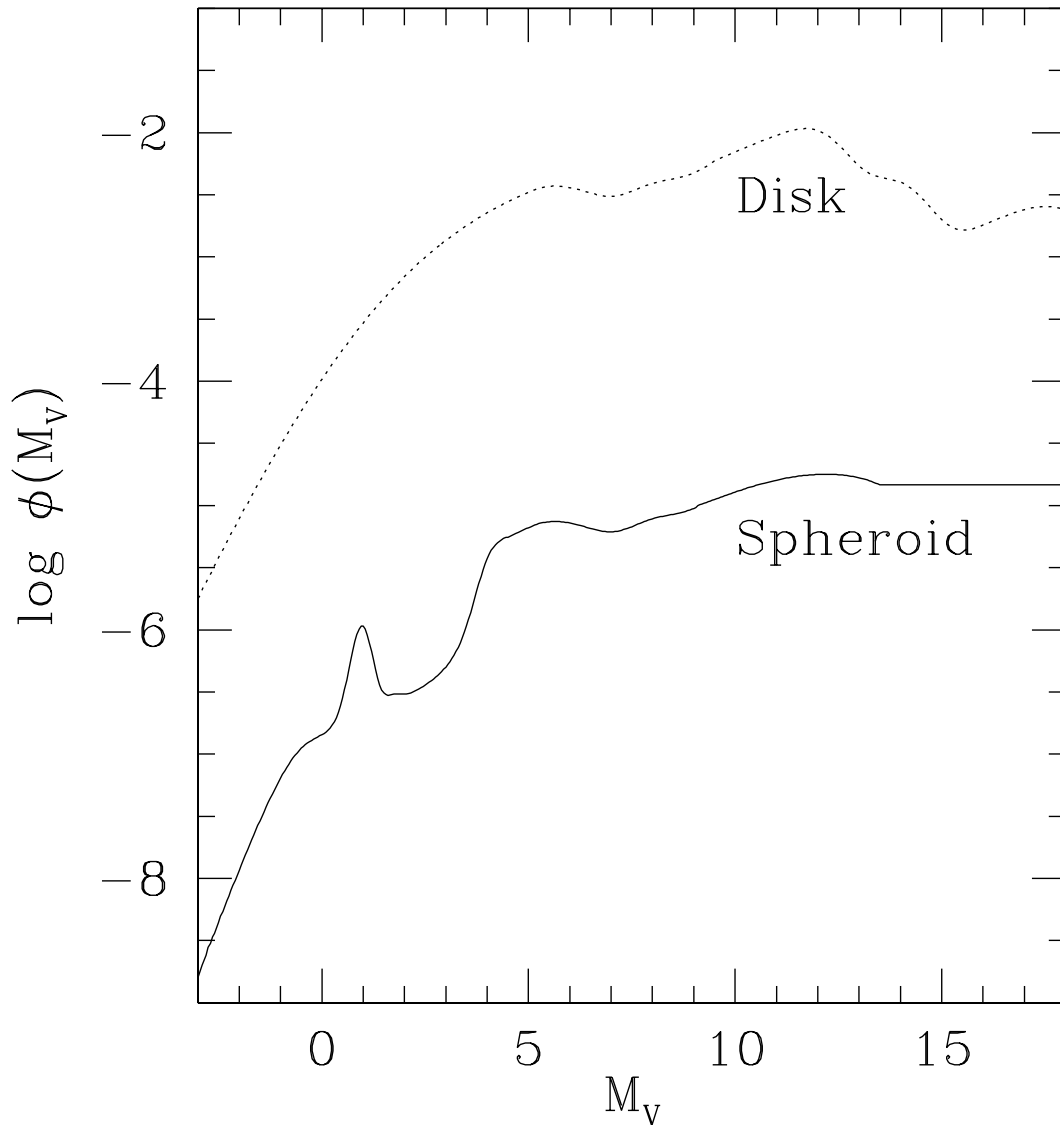


Fig. 1.— The adopted disk and spheroid luminosity functions (LFs). The LFs adopted are the same form those described in Bahcall (1986) except for the following refinements: the disk LF for  $M_V > 9.5$  has been modified to match smoothly the LF derived from *HST* star counts given in Figure 2 of Gould et al. (1997) and the spheroid LF for  $M_V > 7.5$  has been modified to match the LF given in Figure 3 of Gould et al. (1998), also derived from *HST* data.

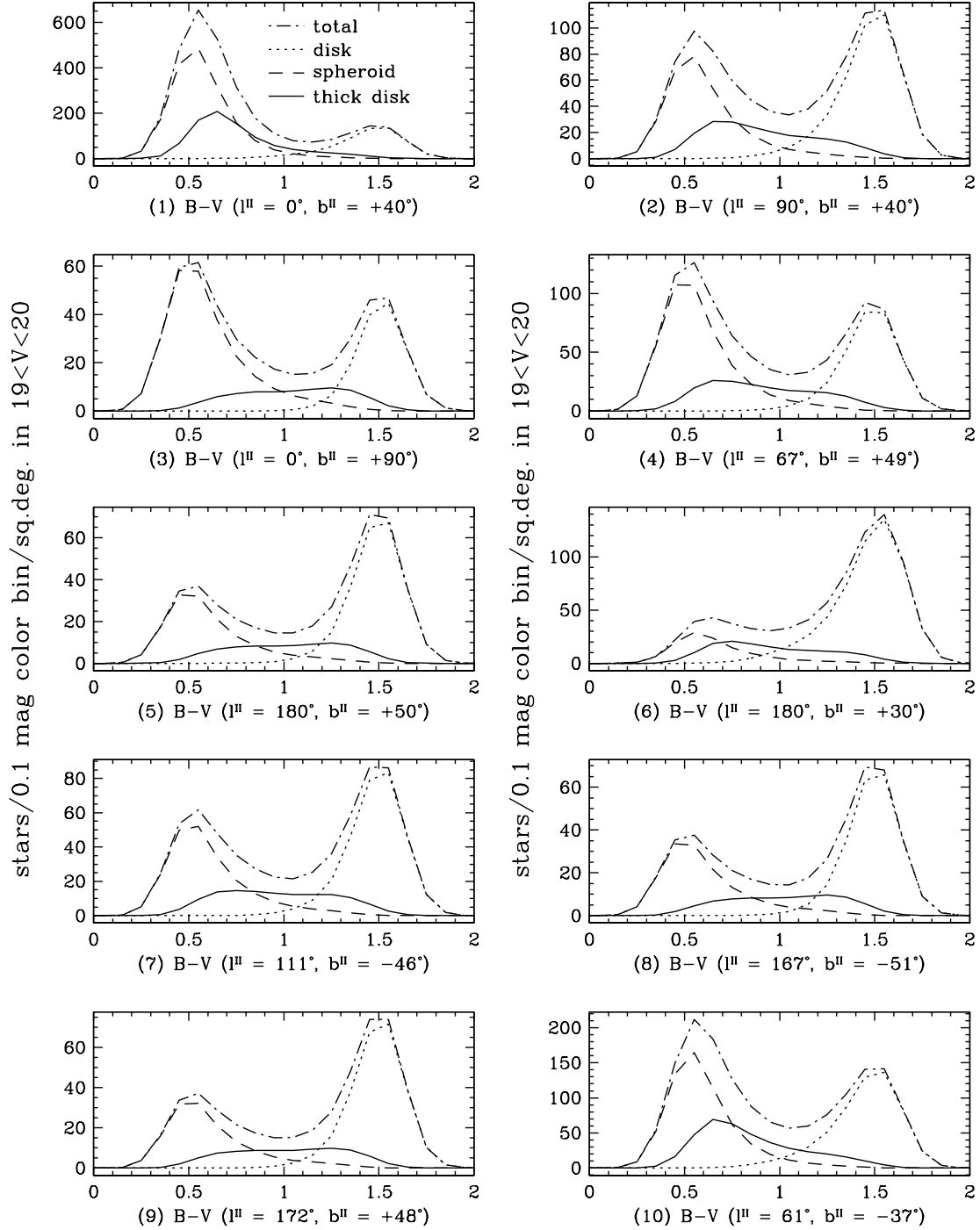


Fig. 2.— Frequency distribution of star colors for a “standard” model (500 : 1, 0.8) (Bahcall 1986) plus a thick-disk as described in § 2, in the apparent magnitude range  $19 < V < 20$ .

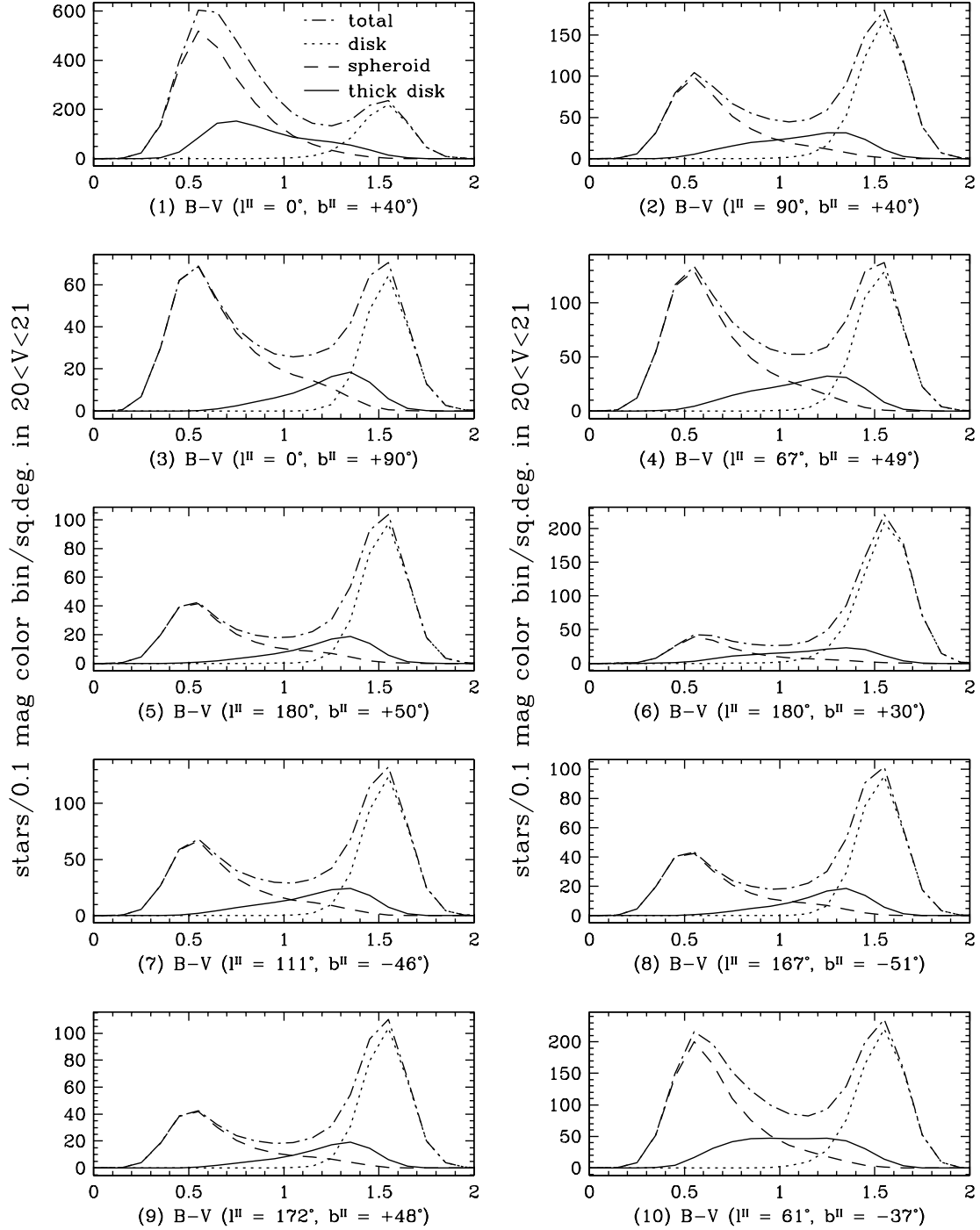


Fig. 3.— Frequency distribution of star colors for a “standard” model (500 : 1, 0.8) (Bahcall 1986) plus a thick-disk as described in § 2, in the apparent magnitude range  $20 < V < 21$ .